N70-10043

Report of the First Year's Work for Contract NAS 9-8869: "Support-Studies for the Coronagraph Contamination Experiment"

Period: September 1, 1968 to August 31, 1969

Principal Investigator: Natalie S. Kovar, Physics Department, University of Houston, Houston, Texas

A. Introduction

In compliance with the contract terms, the four tasks delineated for the first year of the contract were met. These were:

1. Calculation of the Mie scattering functions for a mixture of particles having a range in α between 2 and 240 where α is 2π times the ratio of particle size, r, to wavelength of incident light, λ.
2. Revision of a previously existing computer program for the calculation of Mie scattering functions so as to reduce as far as possible demands on computer memory, storage and time.
3. Computation of Mie scattering functions for uniform size particles, in particular, for particles 15Å in radius.
4. Calculation of Mie scattering functions in the ultraviolet.

Since the enormity of computer data obtained prohibits its inclusion in a report of this type, the following sections will describe the work done in the four above-mentioned areas and present a sampling of the results obtained. The final section will summarize the results to date. In all cases a deck compatible to the Manned Spacecraft Center's Univac 1108 and written in Fortran V is available. Any data will be furnished upon request.

B. Work Description

1) Mie Scattering Functions for a Range in Particle Size

During the contract period, the relative Mie scattering functions, $\sigma'(\theta)$ - where θ is the scattering angle - were computed for spherical particles having an index of refraction m and a size distribution $n(r) \propto r^{-k}$, r being particle size and k the distribution function. The total scattering function is related to the relative scattering function by

$$\sigma(\theta) = C \int_{\alpha_{min}}^{\alpha_{max}} [i_1(\alpha,\theta) + i_1(\alpha,\theta)]\alpha^{-k} \, d\alpha$$

where α is defined above, C is a normalizing factor and i_1 and i_2 are the individual particle scattering functions as described under sections 3) and 4).

Figure 1 shows the relative scattering function for a distribution of 12 to 120 in alpha with the index of refraction equal to 1.33 and the distribution function to 2.5 using increments of 0.10 in alpha. For this distribution, that is, $n(r) \propto r^{-2.5}$, the smallest particles are the most numerous. The range in α corresponds to a particle size range of 1 to 10 microns for a wavelength of 5300Å. It was thought that for these studies which are being done in support of the coronagraph contamination experiment this was approximately the size range of interest (see "Light Scattering by Manned Spacecraft Atmospheres" N. S. Kovar, R. P. Kovar and G. P. Bonner, Planetary and Space Science, Volume 17, p. 143, 1969). For particles of size much smaller than 1μ, the scattering would approach Rayleigh scattering and particles much larger than 10μ would tend to scatter as random individuals and would not contribute appreciably to the general background radiance to be measured by this experiment.

Figure 2 shows the relative scattering functions for the same distribution function and index of refraction but for a particle distribution in alpha of 12 to 240. This means that the particles range in size from 1 to 20μ for a wavelength of 5300Å or from 0.5 to 10μ for a wavelength of 2500Å. Notice this curve and the previous one are quite similar even in scale. This supports the previous statement that larger particles contribute little to the general background radiance. And, too, the assumed particle distribution favors small particles.

2) Revision of Computer Program

The nature of our problem of the calculation of Mie scattering functions, whether for individual particles or a range in particle size, places stringent demands on computer memory, storage and time. For example, whereas the scattering curve for a 15Å particle takes about one minute to calculate on the 1108, that for a 1 cm particle takes in excess of 6 hours computational time for a wavelength of 5300Å. The problem is worsened by using shorter wavelengths since the shorter the wavelength of incident light, the larger the value of alpha for a given particle size.

Figure 3 shows the scattering curve for a 10μ particle for incident light of 1800Å for a range in scattering angle of 0° to 60°. Figures 4 and 5 show the same scattering function for a range of scattering angle of 60° to 120° and 120° to 180°, respectively. To get the exact scattering curve, that is, to include each and every maximum and minimum, it was necessary to take increments of about 0.2 in the scattering angle for this 10 micron particle. It was found that as the particle size is increased by a factor of 10, the increment in scattering angle must be decreased by a corresponding factor of 10 resulting in amplification of computer time needed. Consequently, a sampling technique, described below, was devised.

The program for the calculation of the scattering function for a column of particles having a range in particle size, as described in 1), requires further improvement. The present program does indeed work but further revisions are necessary to reduce computational times. At present, it requires about 50 minutes of 1108 time to compute the scattering function for a range of 2 to 240 in α. Usage of tape for the storage of individual scattering functions, the determination of the optimum accuracy needed in the calculation of individual scattering functions as well as the optimum increment in alpha are all being investigated as means of reducing computer time.

3) Mie Scattering Functions for Uniform Size Particles

For the spacecraft contamination problem, scattering functions for spherical ice particles have been calculated. The range in particle size considered is 15Å to 1 cm and the wavelength range for incident light is 1000Å to 5300Å.

Figures 6 to 8 show the scattering curves for a 15Å particle. The first of these is for incident light of 5300Å, representative of visible wavelengths. Here the index of refraction is 1.33. The ordinate is the log of the scattering function and the abscissa the scattering angle. The next figure shows the curve for the middle ultraviolet represented by 2500Å where the index of refraction is 1.346. Here σ_1 is the scattering function for the component of the incident plane wave having its electric vector perpendicular to the plane of vision and σ_2 that for the electric vector parallel to the plane of vision. $\overline{\sigma}$ is the average of the two. The third figure of this series for a 15Å particle shows the scattering curve for 1200Å which is in the vacuum ultraviolet near the Lyman α line. The index of refraction is complex and equal to 1.353-0.4414i. Note that the shape of the curve is the same at all three wavelengths; that is, it is smooth and has a pronounced minimum at 90° for σ_2.

The next figure, Figure 9, gives the scattering curves for a 1μ size particle for incident light of 5300Å, represented by the solid line, and of 2500Å, represented by the dashed line. The two curves are similar consisting of many maxima and minima and differ markedly from those for 15Å. For small scattering angles, $\theta<10°$, the values of the scattering function at the two wavelengths differ significantly, but for larger scattering angles the scattering functions have approximately the same value.

As explained above, for larger particles machine time becomes prohibitive. Consequently, for the larger particles, 10 or more microns, an averaging or sampling technique was devised and the value of the scattering function computed at selected values of the scattering angle. The procedure used was to compute the scattering function at certain specified intervals in theta. Then, at each of these values the scattering function was calculated at a selected number of adjacent angles and the average scattering function computed for the proscribed range in scattering angle. The exact number of additional thetas and their spacing was governed by previous experience; that is, it was known a priori where the curve was likely to average out as nearly linear and where it would exhibit more erratic behavior. Figure 10 compares the actual and sampled values of $\overline{\sigma}$ for a 10 micron particle at 5300Å. The solid line gives the sampled values and the x's the actual values as taken from the detailed scattering curve. The agreement was found to be good. Even utilizing this sampling technique, however, it took four hours of machine time to obtain the sampled curve for a 1 cm particle at a wavelength of 2500Å using increments of 10° in theta.

Figure 11 gives the curves for a 1000μ particle at 5300Å. Since this figure shows sampled curves, the many maxima and minima of the detailed curves have been smoothed out but their essential shapes have been retained.

Figure 12 shows the curve for a 10,000 micron particle for incident light of 5300Å. The same general shape as for the smaller particles is retained, but the maxima are more rounded and less pronounced.

4) Mie Scattering Functions for Ultraviolet Incident Light

Some scattering functions for incident light having a wavelength in the ultraviolet have been presented above. No difficulties were encountered in calculating the scattering functions for ice particles for wavelengths $\geq$ 1800Å. However, for wavelengths shorter than 1800Å, the index of refraction for ice becomes complex which introduces somewhat more difficulty into the computation. The computer program was successfully altered to accomodate complex indices of refraction and Mie scattering functions were computed for ice particles for which the wavelength of incident light was as short as 1000Å. Some of these are presented below.

The curve for a 1 micron particle at 1200Å is shown in Figure 13. Here the index of refraction is complex and it is to be noted that the curve differs from that for the same size particle at 5300Å and 2500Å, as shown in Figure 9, in that it damps out at about 50°.

Figure 14 shows the sampled curve for a 100μ particle for incident light of 2500Å. Note that there are strong secondary maxima at about 120° and at 140°. The maximum at 140° is typical of ice particles.

As the next figure, Figure 15, indicates, when the index of refraction becomes complex, as it does for a wavelength of 1200Å, the scattering curve exhibits a substantially different behavior than when the index of refraction is real. These curves are for a 10μ particle. σ_1 no longer has a pronounced maximum at 140° but increases slowly to a maximum at 100°; σ_2 has a rather broad maximum from 60° to 90°.

Figure 16 shows the sampled scattering curve for a 1 cm particle for incident light of 2500Å.

C. Other Activities

As a result of the work done on this contract, a paper was submitted to the Hawaii meeting of the American Astronomical Society. An abstract of this paper is to appear in a forthcoming issue of the Bulletin of the American Astronomical Society.

Secondly, a NASA sponsored workshop on optical technology held in Huntsville, Alabama was attended. The problems of contamination were a point of discussion at this meeting.

Lastly, an invited paper entitled "Theory of Light Scattering by Manned Spacecraft Atmospheres" was presented at the Symposium for Optical Contamination held in Aspen, Colorado by the Rocky Mountain Section of the Optical Society of America, August 1969.

D. Summary of Available Mie Scattering Functions for Ice Particles

1) Individual Particles

Wavelength of Incident Light	Particle Sizes
5300Å, 2500Å, 1800Å	15Å, 1μ, 10μ, 100μ, 1000μ, 10,000μ
1700Å, 1600Å, 1500Å, 1400Å 1300Å, 1200Å, 1100Å, 1000Å	15Å, 1μ, 10μ, 100μ, 1000μ

2) Particle Size Distribution

α: 2 to 120 and 12 to 120, with $m = 1.30$, $k = 3.0$ and $m = 1.33$, $k = 2.5$

α: 2 to 120 and 12 to 120, with $m = 1.30$, $k = 3.0$ and $m = 1.33$, $k = 2.5$

FIGURE 1

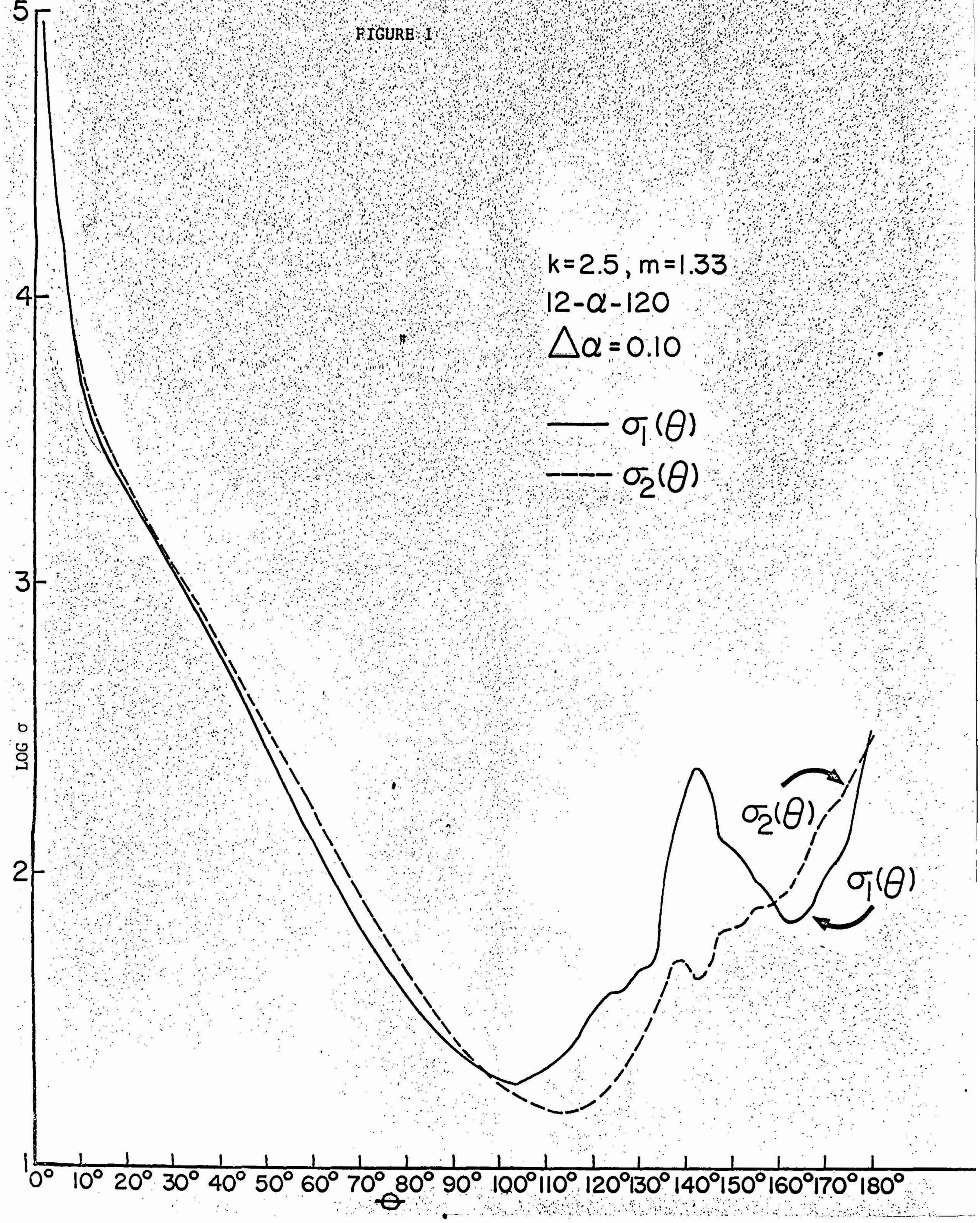

k=2.5, m=1.33
12-α-120
Δα=0.10
σ1(θ)
σ2(θ)
σ2(θ)
σ1(θ)
LOG σ
5
4
3
2
1
0° 10° 20° 30° 40° 50° 60° 70° 80° 90° 100° 110° 120° 130° 140° 150° 160° 170° 180°
θ

FIGURE 2

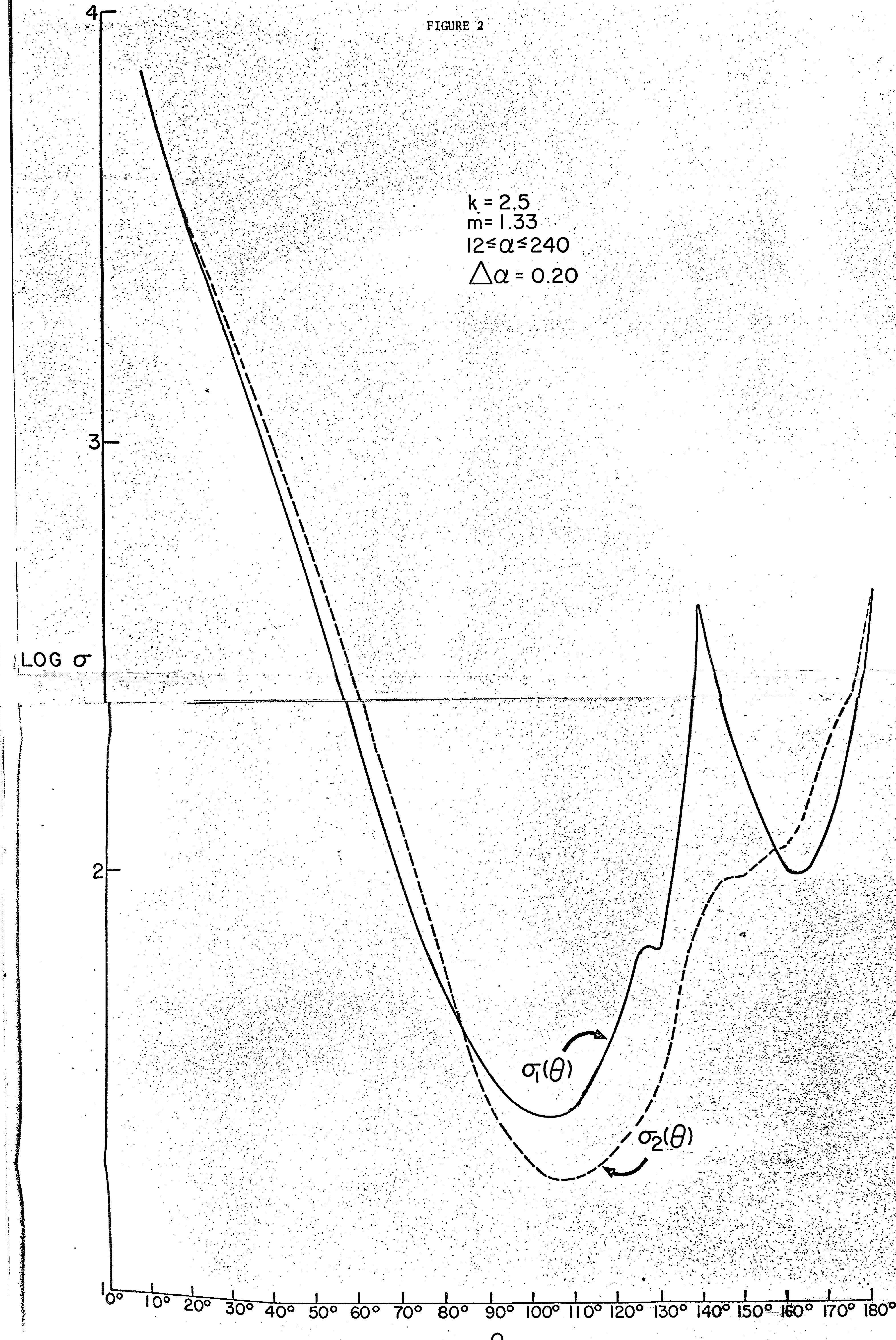

k = 2.5
m= 1.33
12≤α≤240
Δα = 0.20
σ1(θ)
σ2(θ)
LOG σ
4
3
2
1
0° 10° 20° 30° 40° 50° 60° 70° 80° 90° 100° 110° 120° 130° 140° 150° 160° 170° 180°
θ

FIGURE 3

MIE SCATTERING FUNCTION

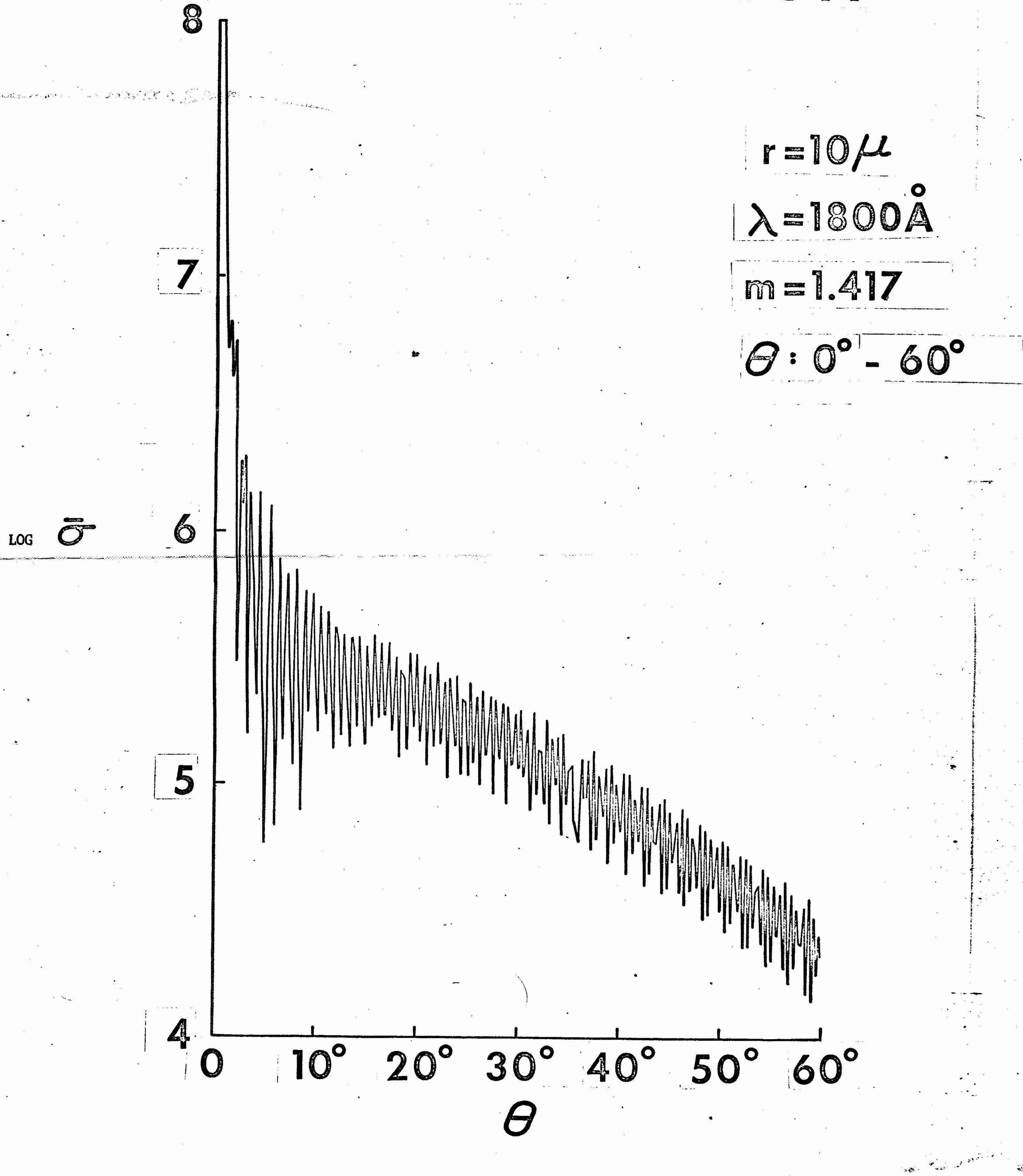

FIGURE 4

MIE SCATTERING FUNCTION

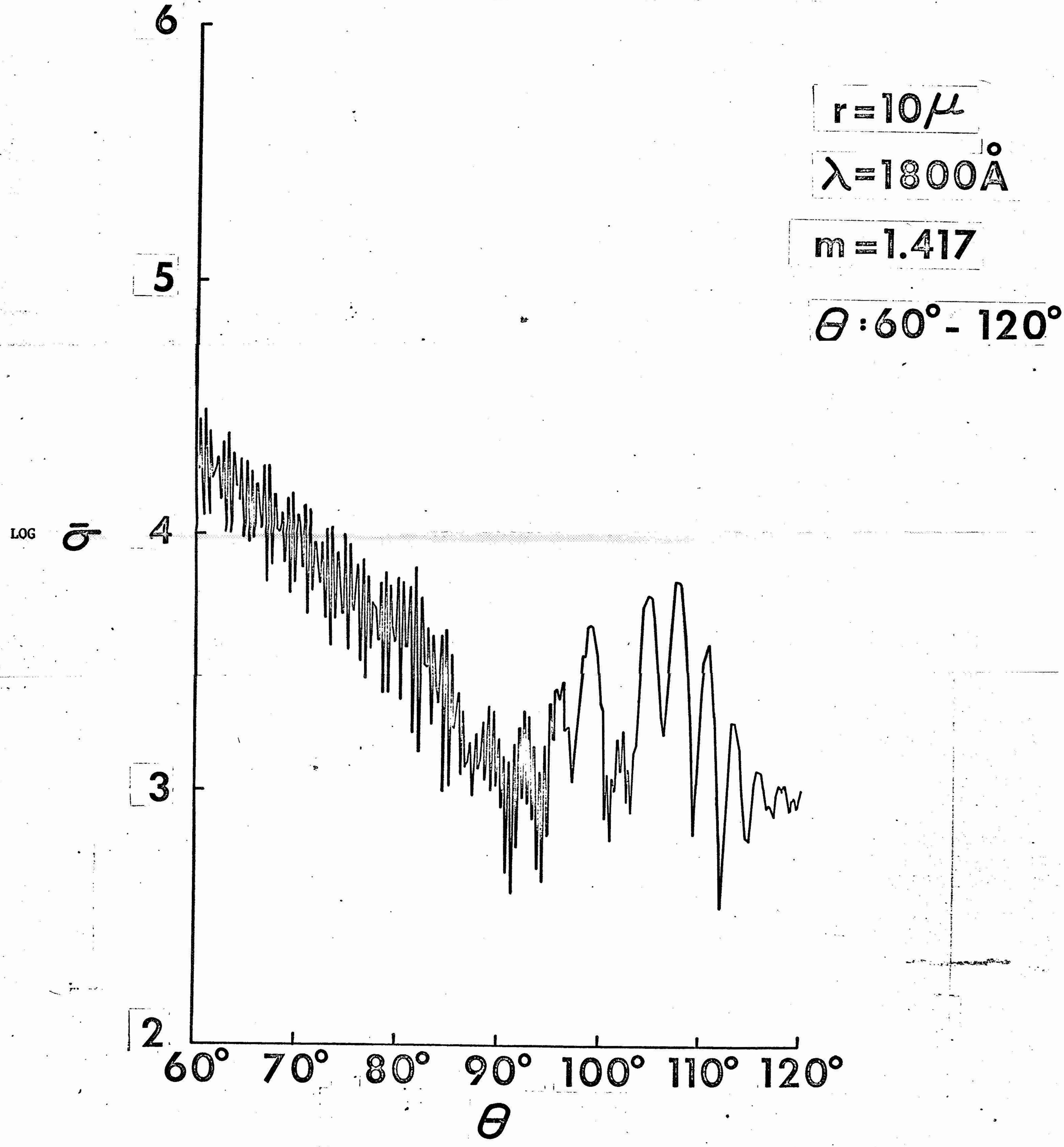

FIGURE 5

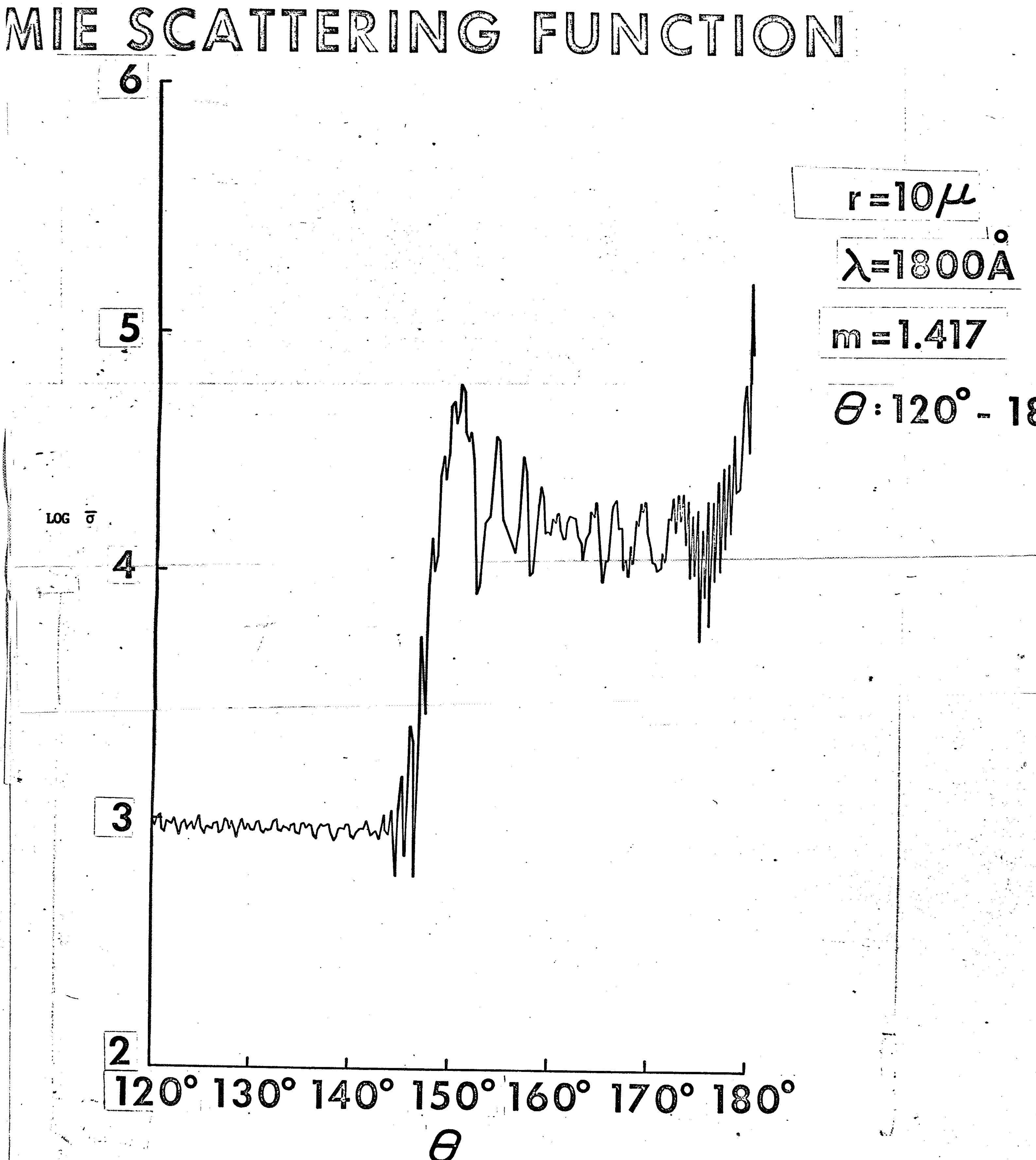
MIE SCATTERING FUNCTION
6
5
4
3
2
LOG $\overline{\sigma}$
r = 10μ
λ=1800Å
m = 1.417
θ: 120° - 18
120° 130° 140° 150° 160° 170° 180°
θ

FIGURE 6

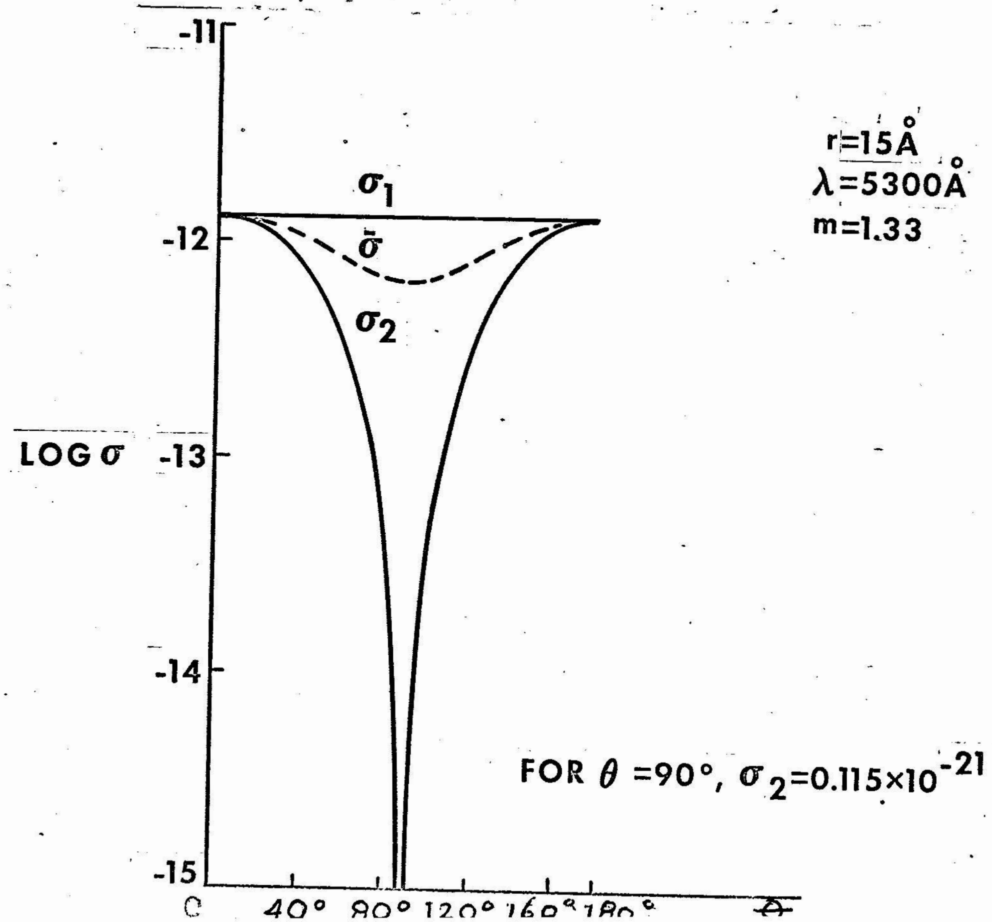

-11
-12
-13
-14
-15
LOG σ
σ1
σ̄
σ2
r=15Å
λ=5300Å
m=1.33
FOR θ =90°, σ 2=0.115×10-21
40°
80°
120°
180°
θ

FIGURE 7

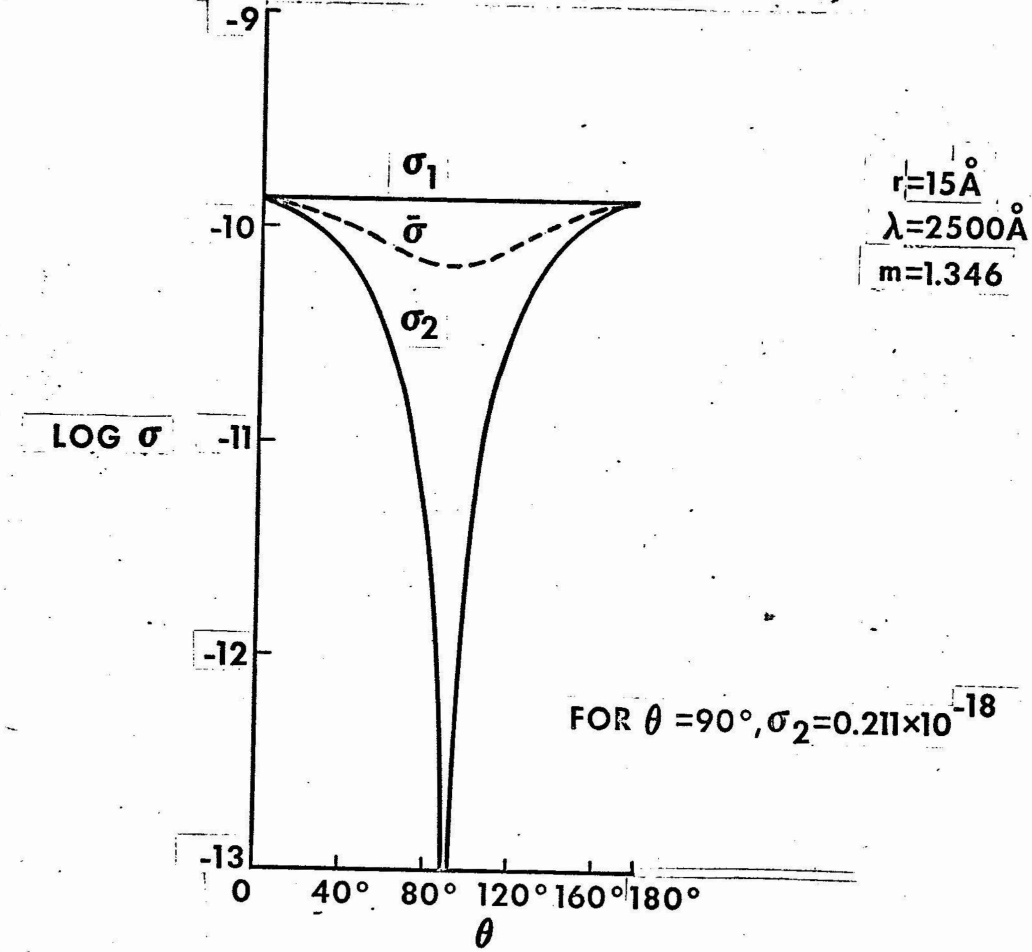

-9
-10
-11
-12
-13
LOG σ
σ1
σ̄
σ2
r=15Å
λ=2500Å
m=1.346
FOR θ =90°, σ2=0.211×10-18
0
40°
80°
120°
160°
180°
θ

FIGURE 8

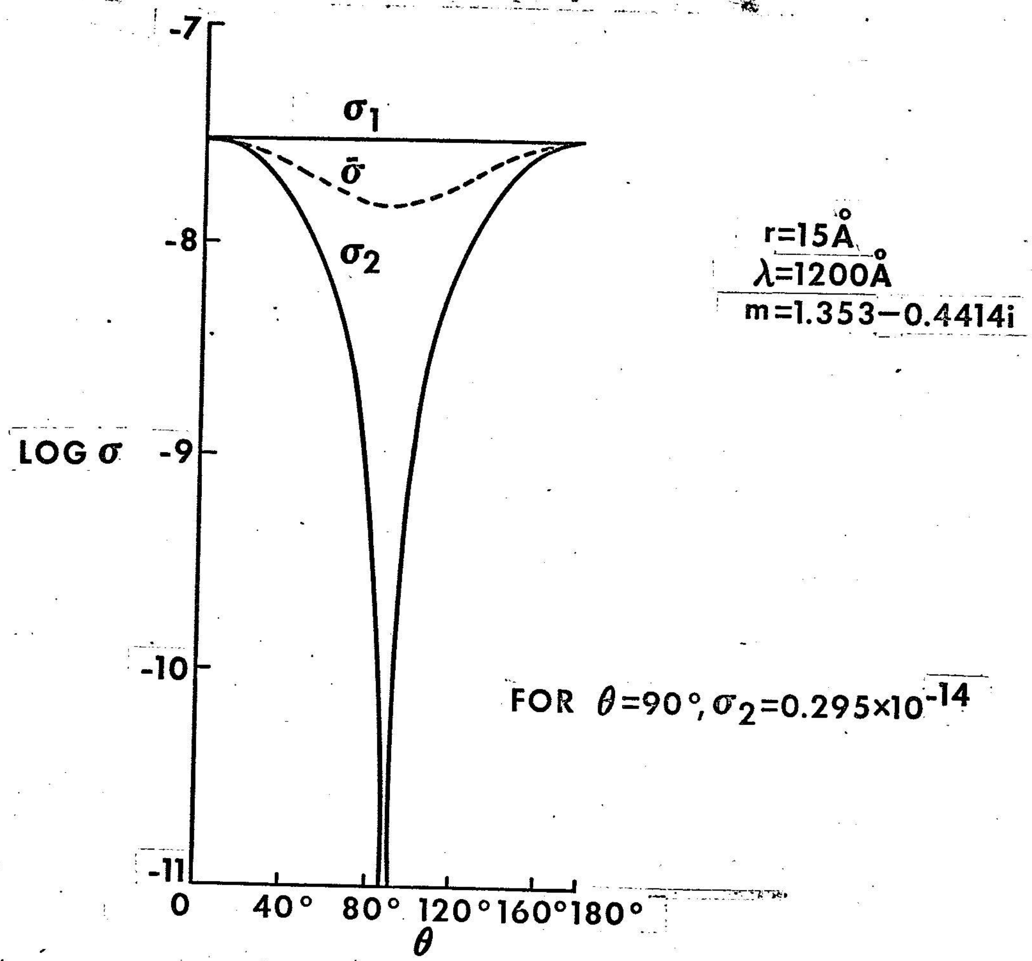

-7
-8
-9
-10
-11
LOG σ
σ1
σ̄
σ2
r=15Å
λ=1200Å
m=1.353−0.4414i
FOR θ=90°, σ2=0.295×10^-14
0
40°
80°
120°
160°
180°
θ

FIGURE 9

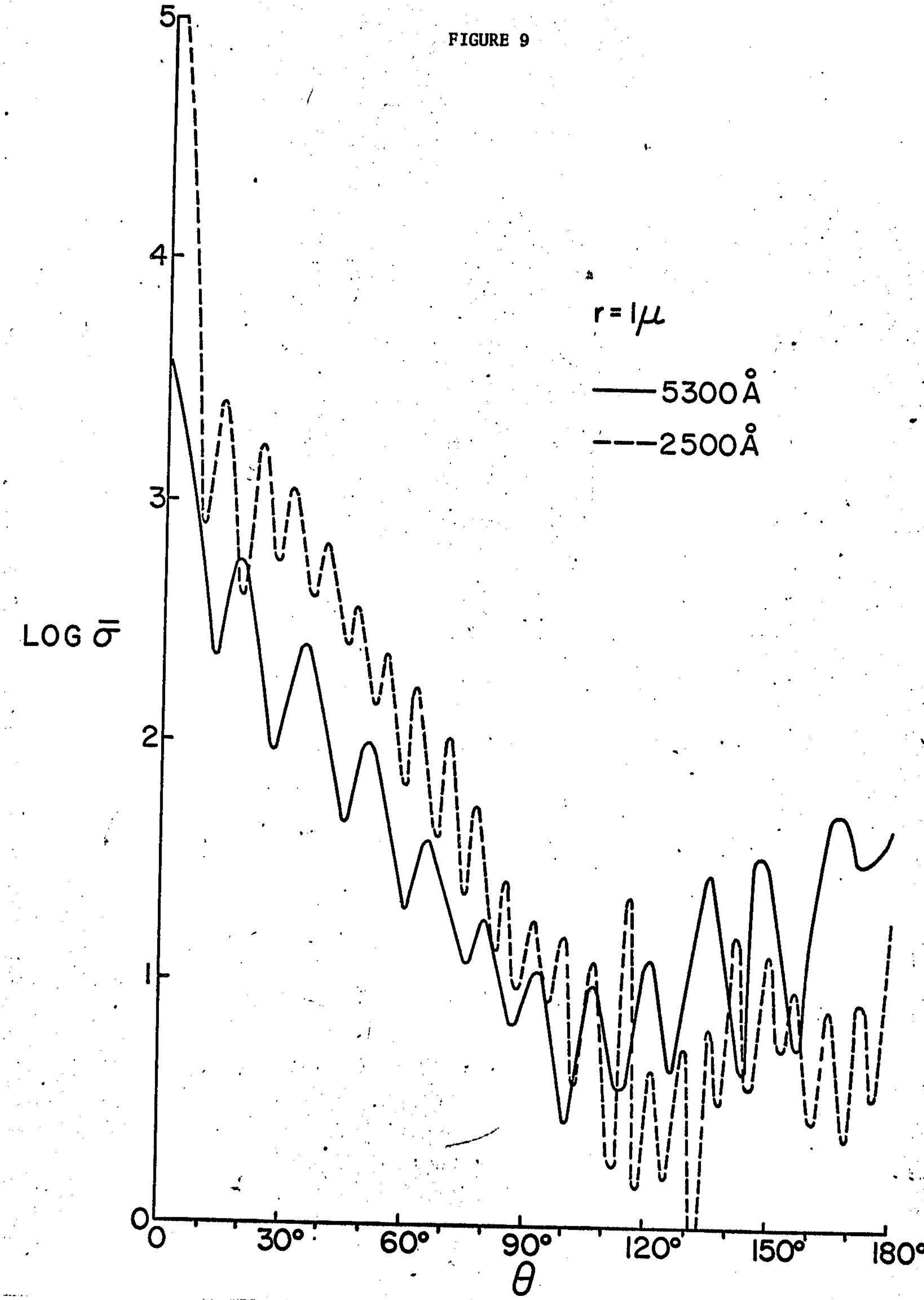

FIGURE 10

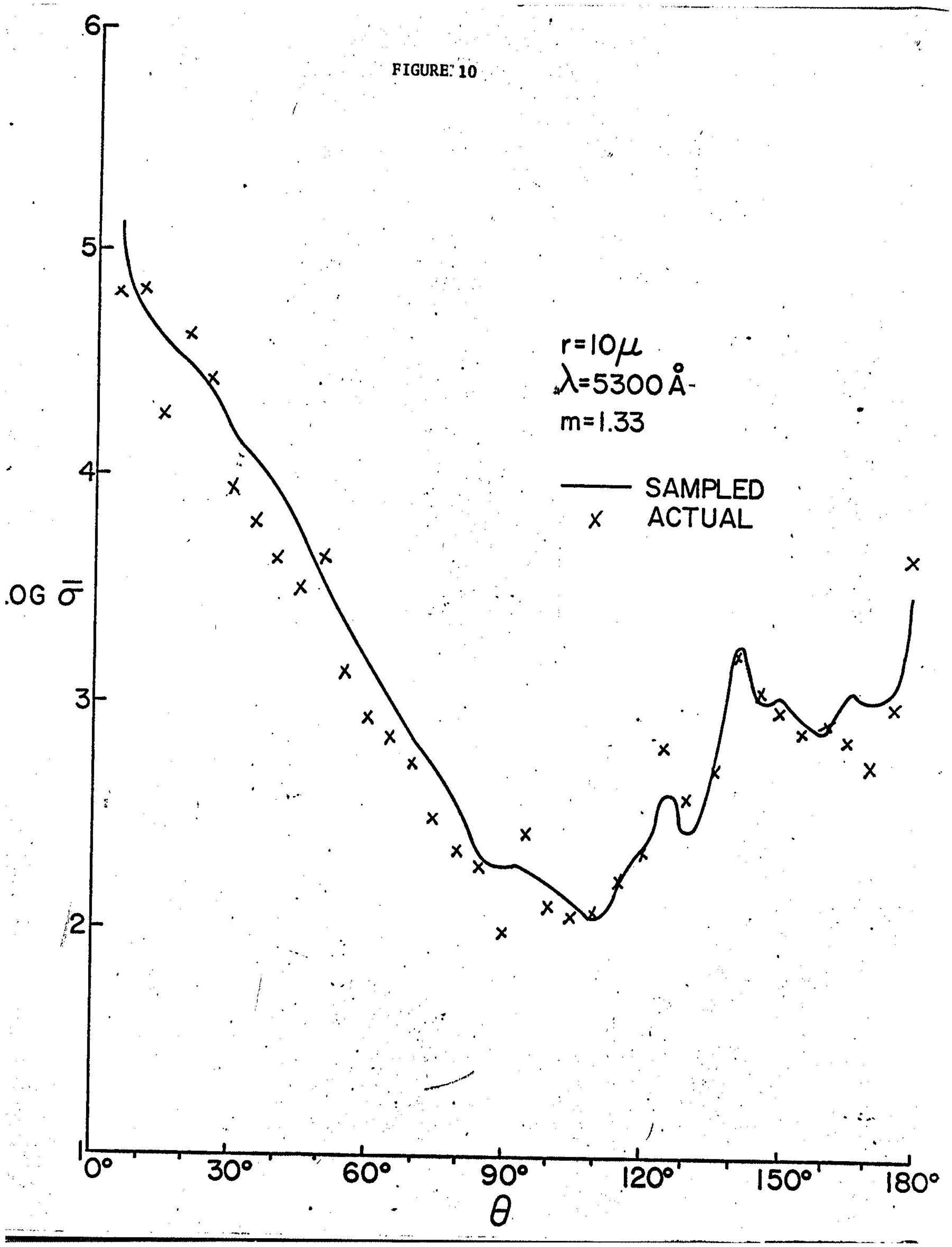

r=10μ
λ=5300 Å
m=1.33
SAMPLED
ACTUAL
.OG σ̄
6
5
4
3
2
1
0°
30°
60°
90°
120°
150°
180°
θ

FIGURE 11

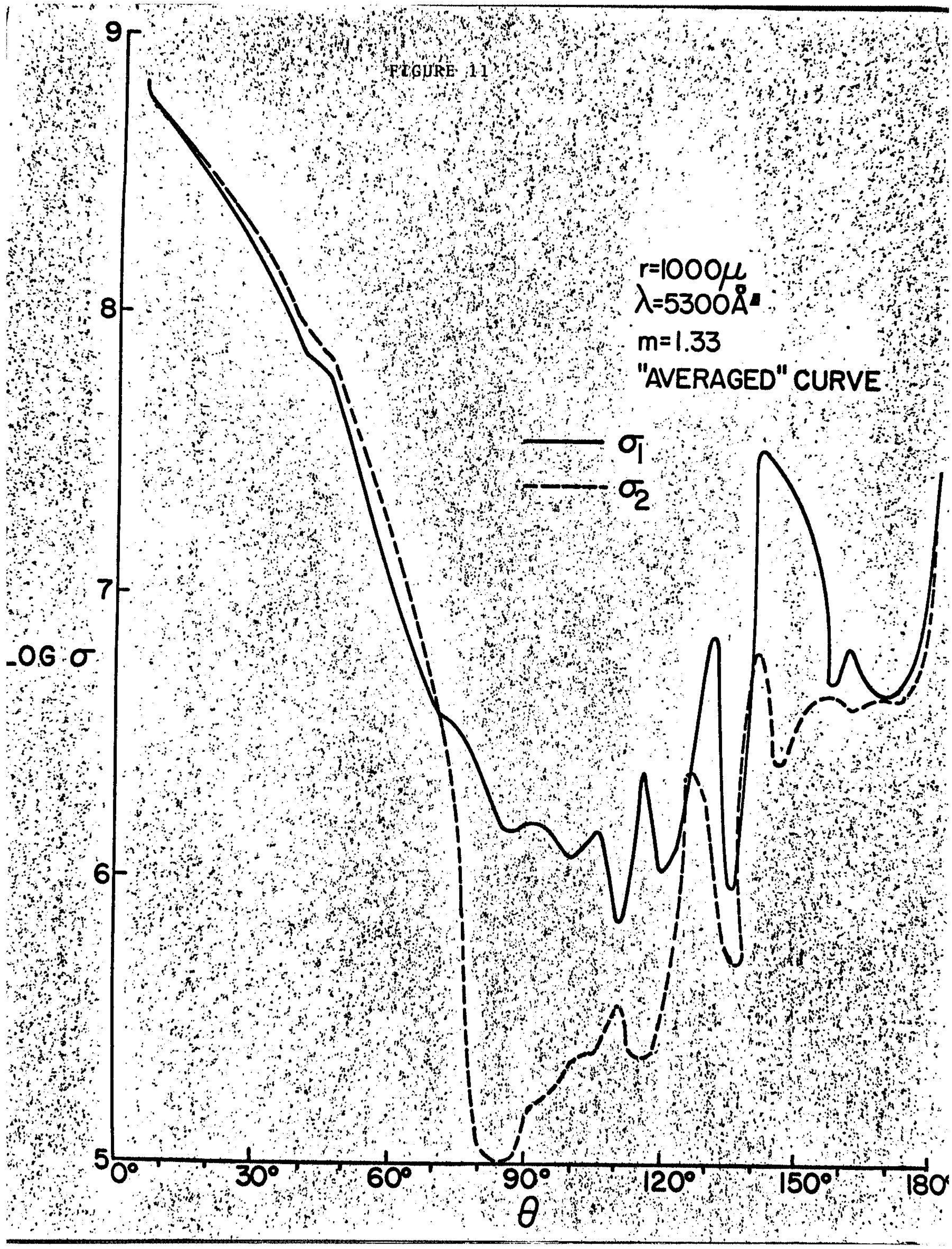

r=1000μ
λ=5300Å
m=1.33
"AVERAGED" CURVE
σ1
σ2
LOG σ
9
8
7
6
5
0°
30°
60°
90°
120°
150°
180°
θ

FIGURE 12

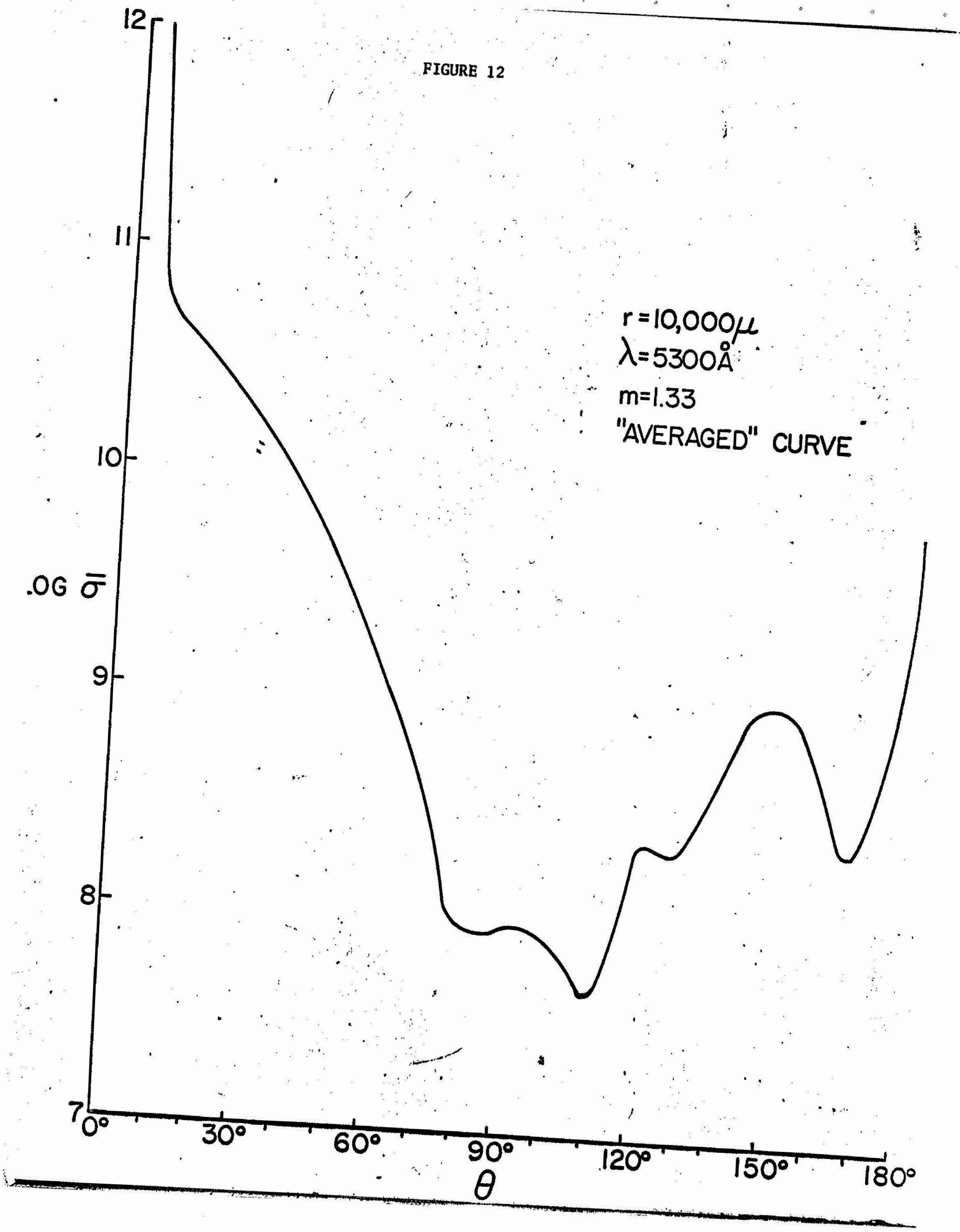
r = 10,000μ
λ=5300Å
m=1.33
"AVERAGED" CURVE
.OG σ̄
12
11
10
9
8
7
0°
30°
60°
90°
120°
150°
180°
θ

FIGURE 13

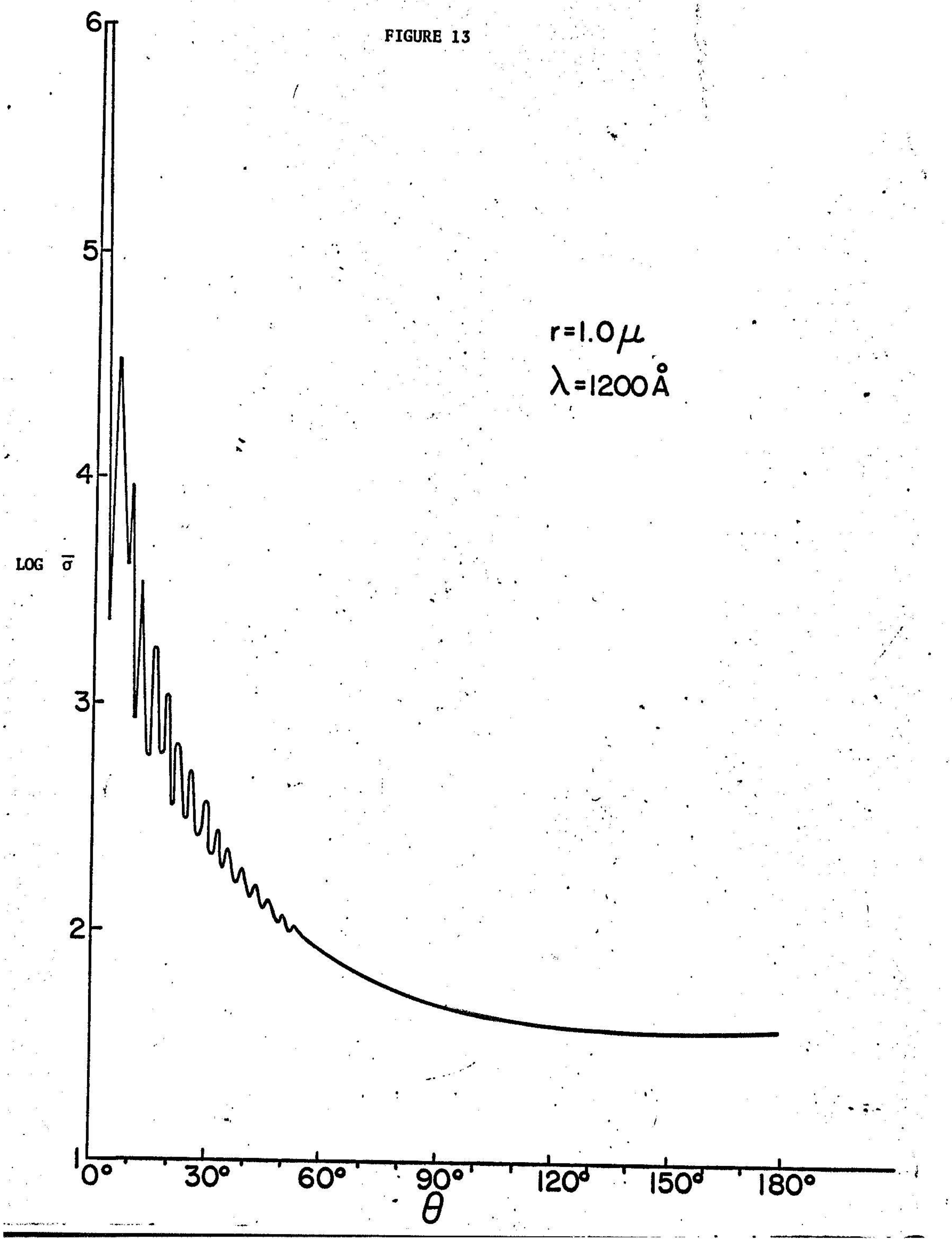

FIGURE 14

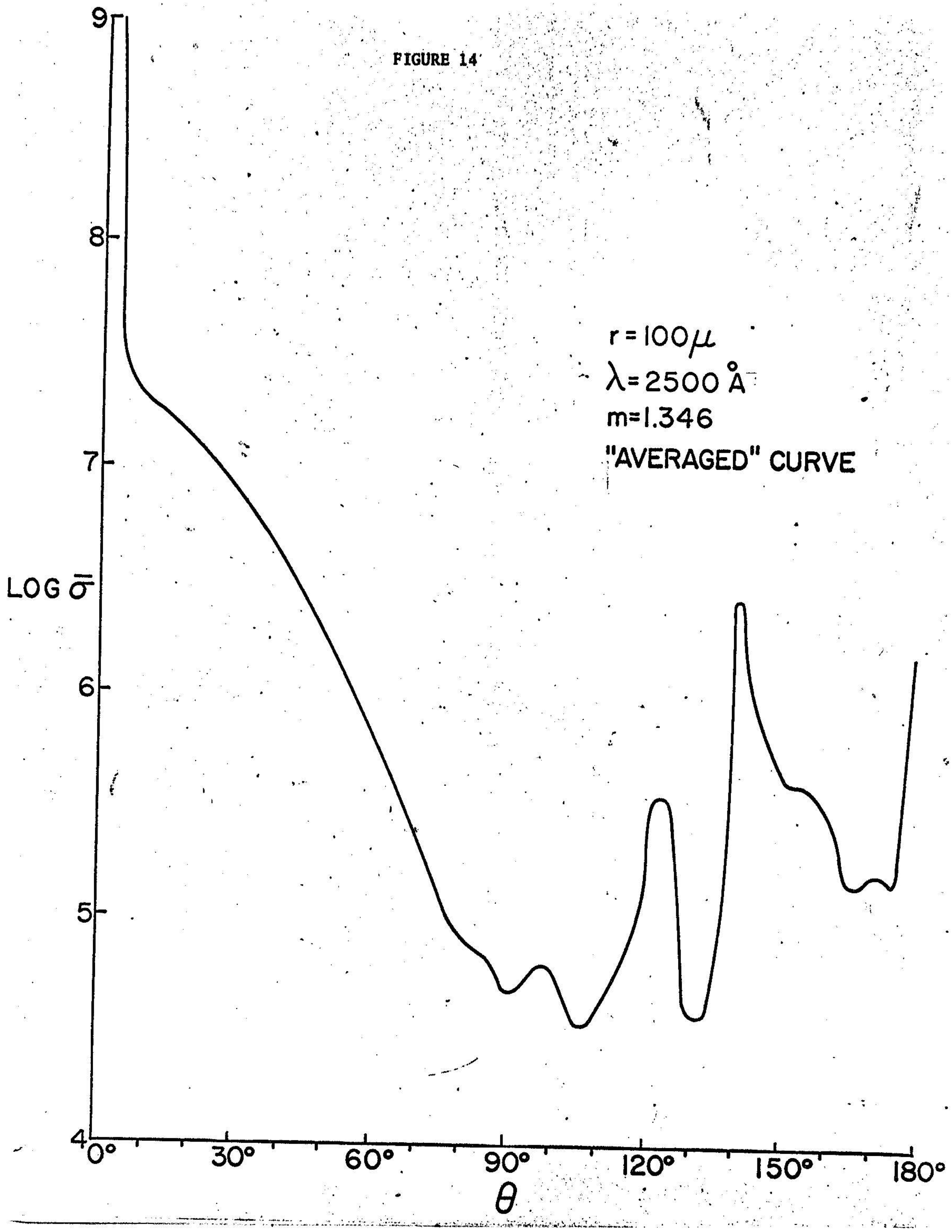

r = 100μ
λ= 2500 Å
m=1.346
"AVERAGED" CURVE
LOG σ̄
9
8
7
6
5
4
0°
30°
60°
90°
120°
150°
180°
θ

FIGURE 18

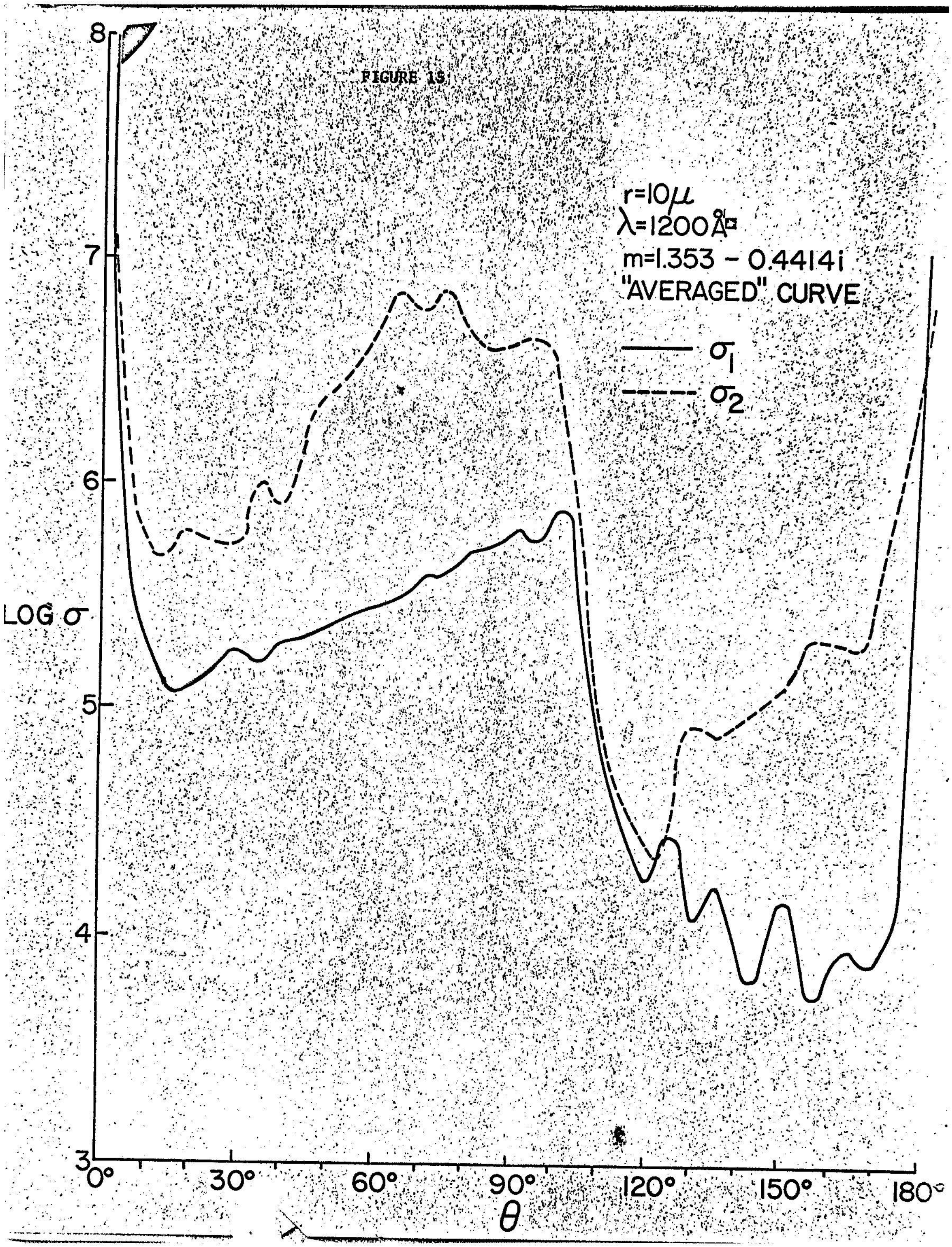
r=10μ
λ=1200Å
m=1.353 - 0.4414i
"AVERAGED" CURVE
σ1
σ2
LOG σ
8
7
6
5
4
3
0°
30°
60°
90°
120°
150°
180°
θ

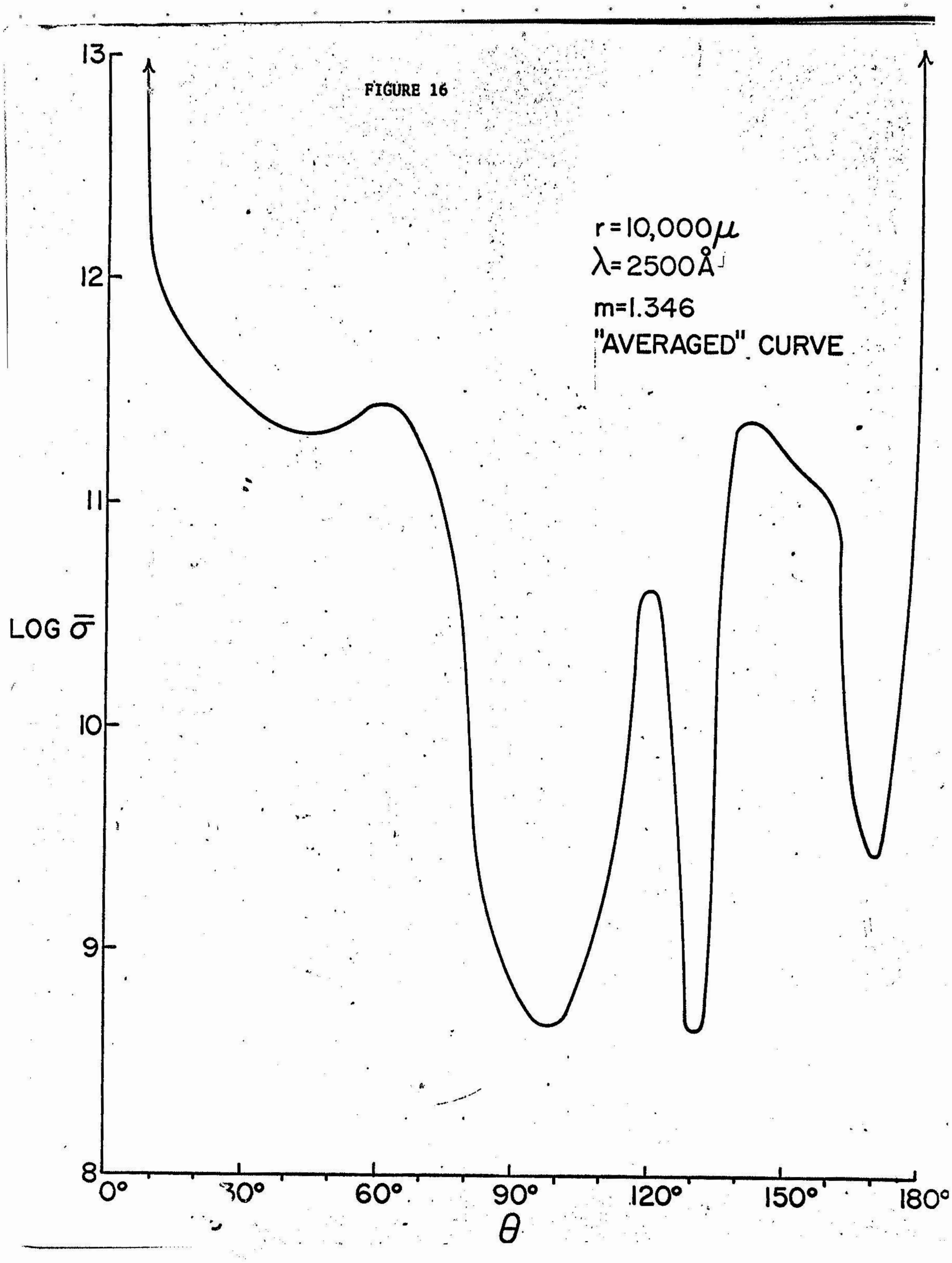
FIGURE 16
r = 10,000 μ
λ = 2500 Å
m = 1.346
"AVERAGED" CURVE
LOG σ̄
13
12
11
10
9
8
0°
30°
60°
90°
120°
150°
180°
θ